

Ⅲ. 研究成果の刊行物・別刷

Gallstones increase the prevalence of Barrett's esophagus

Juntaro Matsuzaki · Hidekazu Suzuki ·
Keiko Asakura · Yoshimasa Saito · Kenro Hirata ·
Toru Takebayashi · Toshifumi Hibi

Received: 7 July 2009 / Accepted: 7 October 2009 / Published online: 12 November 2009
© Springer 2009

Abstract

Purpose Bile and acid exposures are thought to be major risk factors for Barrett's esophagus in Western countries. The association of gallstones with Barrett's esophagus has not been fully evaluated. The present study was designed as a case-control study for determining the possible factors associated with endoscopically suspected esophageal metaplasia (ESEM), defined as an endoscopic finding suggestive of Barrett's esophagus, in Japanese patients.

Methods A total of 528 patients with ESEM were allocated to the case group, while 528 age- and gender-matched patients without ESEM were allocated to the control group. Findings on esophagogastroduodenoscopy and clinical background factors were compared using a multivariate logistic regression model.

Results The presence of gallstones and hiatus hernia and the severity of gastric mucosal atrophy were independently associated with the presence of ESEM [odds ratio (OR) **1.67**, 95% confidence interval (CI) 1.03–2.69; OR **2.75**, 95% CI 1.75–4.33; OR **1.25**, 95% CI 1.01–5.6, respectively]. Compared with subjects with neither gastric corpus atrophy nor gallstones, although subjects with gallstones alone were not associated with the presence of ESEM (OR **1.59**, 95% CI 0.87–2.92), having both gastric corpus

atrophy and gallstones was strongly associated with the presence of ESEM (OR **2.94**, 95% CI 1.40–6.17).

Conclusions The presence of gallstones was independently associated with the presence of ESEM in the Japanese outpatient population, suggesting a causal association of distal esophageal bile exposure with the development of ESEM. Further studies are needed to confirm our findings in cases with histologically confirmed Barrett's esophagus.

Keywords Barrett's esophagus · ESEM · Gallstone · Gastric mucosal atrophy

Introduction

The incidence of esophageal adenocarcinoma is rising more rapidly than that of any other malignancy in Western countries [1–3]. Esophageal adenocarcinoma remains highly lethal, with a 5-year survival rate of less than 15% [4, 5]. In most patients, esophageal adenocarcinoma arises from its premalignant precursor lesion, Barrett's esophagus (BE) [6]. BE is a transformation of the esophageal squamous epithelium into gastric metaplasia or specialized intestinal metaplasia [7]. Investigating the risk factors of BE was important to clarify the cause of BE and esophageal adenocarcinoma.

BEs are classically attributed to reflux of the acid component of gastric content into the esophagus. Meanwhile, a number of observation support the concept that bile reflux, as occurs in duodeno-gastro-esophageal reflux (DGER), also contributes to the development of BE [8–11]. Izbeki et al. [12] reported that prevalence of gallstone disease was increased and gallbladder motility was impaired in patients with BE. Since microscopic cholesterol crystals are regularly washed out of the gallbladder if

J. Matsuzaki · H. Suzuki (✉) · Y. Saito · K. Hirata · T. Hibi
Division of Gastroenterology and Hepatology,
Department of Internal Medicine, Keio University
School of Medicine, 35 Shinanomachi, Shinjuku-ku,
Tokyo 160-8582, Japan
e-mail: hsuzuki@sc.itc.keio.ac.jp

K. Asakura · T. Takebayashi
Department of Preventive Medicine and Public Health,
Keio University School of Medicine, Tokyo, Japan

its contractions are effective enough, impaired motility of the gallbladder is one of the factors contributing to the development of gallstones [13]. Gallbladder dysfunction or nonfunction is closely associated with the efficiency of continuous bile flow into the duodenum and the occurrence of duodeno-gastric reflux [14, 15]. Therefore, the formation of gallstones has been considered to be associated with duodeno-gastric reflux [16].

According to the Montreal definitions, the term endoscopically suspected esophageal metaplasia (ESEM) is used for an endoscopic finding consistent with BE that awaits histological evaluation [7]. The prevalence of long-segment ESEM, where the length of the circumferential ESEM is more than 3 cm, has been estimated to be 0.2–0.4%, while that of short segment ESEM, where the length of the circumferential ESEM is less than 3 cm, has been estimated to be 6.0–20.6% in Japan [17, 18]. To diagnose for BE, an intensive biopsy protocol of four quadrant biopsies, taken at 1–2 cm intervals, for all patients with ESEM has been recommended [19, 20]. Although histological confirmations are needed to clarify the risk factors for BE, lower esophageal adenocarcinoma is still a rare disease in Japan, and biopsies from sites of ESEM are not routinely obtained at the screening EGD due to cost, risk and complexity. Since the presence of ESEM is a prerequisite condition for the development of BE [21], risk factors for ESEM also extend to BE and esophageal adenocarcinoma.

Several risk factors for BE are reported, such as gastro-esophageal reflux symptoms, hiatus hernia, aging, male gender, obesity, alcohol and tobacco use [22–27]. However, it is unknown whether the presence of gallstones is an independent risk factor for BE. Therefore, the authors performed a multivariate analysis on the relationship between ESEM and gallstones.

Methods

Study population

The authors conducted a hospital-based age- and gender-matched case control study on 4945 patients (2854 male, 2091 female; mean age, 62.6 years; range 13–94 years) who underwent esophagogastroduodenoscopy (EGD) at Keio University Hospital between November 2007 and April 2008. A total of 538 patients were diagnosed as having ESEM (10.8%). We reviewed the medical records and the digital photo image files of the EGD patients. Patients in whom the esophagogastric junction (EGJ) had been resected in a previous operation, such as total gastrectomy, proximal gastrectomy or esophagectomy, and those who had undergone endoscopic mucosal resection

(EMR) or endoscopic variceal ligation (EVL) in the esophagus were excluded. Patients who had undergone distal gastrectomy were not excluded. In addition, patients for whom the EGJ was not recorded in the photo image files of EGD were also excluded. Then patients were excluded among 538 patients with ESEM; 528 patients (356 men and 172 women; mean age, 65.3 years; range 20–87 years) with ESEM were allocated to the case group, while 528 age- and gender-matched (frequency matching) patients without ESEM were allocated to the control group. When the control patients were selected, the medical records and EGD photo images of those patients were also reviewed, and patients who met the exclusion criteria were excluded (Fig. 1). Characteristics of the subjects are shown in Table 1. The study was performed in accordance with the Declaration of Helsinki.

Assessment by endoscopy

The presence/absence of ESEM and hiatus hernia was determined, and gastric mucosal atrophy and reflux esophagitis were graded retrospectively by three gastrointestinal endoscopists according to the criteria listed below.

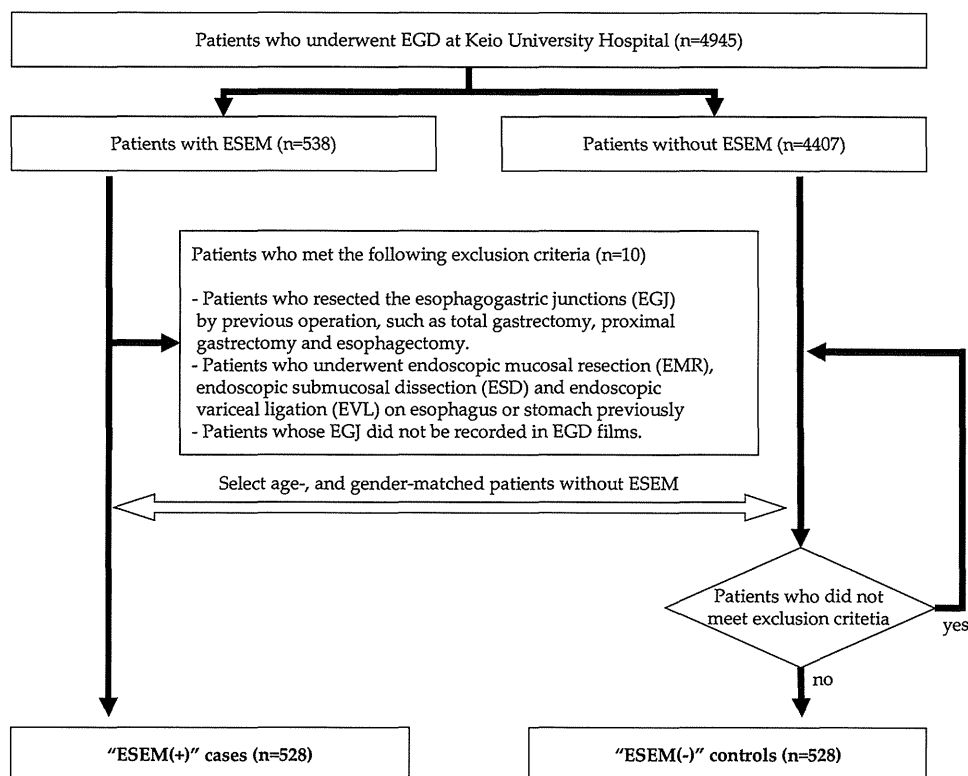
ESEM

The presence/absence of ESEM was examined in the lower portion of the esophagus, including the EGJ, during inflation of the esophagus. The EGJ was defined as the oral side end of the fold continuous with the gastric lumen [28], as well as the anal side end of the palisade vessel, because the veins in the lower part of the esophagus were distributed uniformly, running parallel and longitudinally in the lamina propria [21, 29]. The squamo-columnar junction (SCJ) was defined by a clear change in the color of the mucosa. ESEM was defined as the area between the SCJ and the EGJ [21]. Most patients were evaluated for the presence/absence of ESEM using the anal side end of the lower esophageal palisade vessel, since such a definition of the EGJ was more suitable for the retrospective evaluation.

Gastric mucosal atrophy

The severity of gastric mucosal atrophy was assessed endoscopically by the Kimura–Takemoto classification of the atrophic pattern [21, 30, 31]. This classification divides the severity of gastric mucosal atrophy into seven types (C-0, C-1, C-2, C-3, O-1, O-2 and O-3) according to the location of the atrophic border as detected by endoscopy as follows: C-0, absence of atrophy; C-1, pyloric mucosal atrophy; C-2, atrophy extending over the lesser curvature of the lower third of the stomach; C-3, the atrophy extending over the lesser curvature of the middle third of

Fig. 1 Diagram of the case control study. Among 4945 patients who underwent esophagogastroduodenoscopy (EGD) at Keio University Hospital between November 2007 and April 2008, there were 538 patients with endoscopically suspected esophageal metaplasia (ESEM), defined as an endoscopic finding suggestive of BE, and 4407 patients without ESEM. Among 538 subjects with ESEM, 10 subjects were excluded by the exclusion criteria, and 528 subjects were allocated to the case groups. Then among 4407 subjects without ESEM, 528 subjects were allocated to the control groups. These 1056 cases and controls were reviewed according to the medical records and EGD films, and it was confirmed that these did not meet the exclusion criteria



the stomach; O-1, border of the atrophy between the lesser curvature and anterior wall of the stomach; O-2, atrophy within the limits of the anterior wall of the stomach; O-3, atrophic area extending from the anterior wall to the major curvature of the stomach. Using this classification, the severity of the gastric mucosal atrophy was divided into four grades: none (C-0), mild (C-1 and C-2), moderate (C-3 and O-1) and severe (O-2 and O-3).

Hiatus hernia

The presence/absence of hiatus hernia was examined by the valvular appearance of the cardia visualized from below using the retroflexed endoscope during gastric inflation [32].

Reflux esophagitis

Reflux esophagitis was defined as the presence of gross mucosal injury, ranging from red longitudinal streaks with associated friability to erosion or ulceration in the distal esophagus or breakage in the lower portion of the esophagus. The severity of reflux esophagitis was graded according to the Los Angeles classification [33].

Clinical background factors

The alcohol consumption status, smoking status and the presence/absence of *H. pylori* infection, obesity,

hypertension, diabetes mellitus, dyslipidemia and gallstones were determined from the medical records. The alcohol consumption status was defined as a positive/negative history of daily alcohol consumption. The smoking status was defined as a positive/negative history of smoking cigarettes. The presence of *H. pylori* infection was defined as a history of *H. pylori* infection, including both pre- and post-eradication. The presence of *H. pylori* infection was detected by serological test, ¹³C-urea breath test, culture or histology of the gastric mucosal biopsy specimen. Obesity was defined as a body mass index of more than 25 kg/m². Hypertension was defined as systolic blood pressure of over 140 mmHg and/or diastolic blood pressure of over 90 mmHg, or a history of use of antihypertensive drugs for the treatment of hypertension. Diabetes mellitus was defined as a serum hemoglobin A_{1c} (HbA_{1c}) value of over 6.5% or a history of use of antidiabetic agents. Dyslipidemia was defined as a serum level of low-density lipoprotein cholesterol (LDL-C) of over 140 mg/dl, high-density lipoprotein cholesterol (HDL-C) of under 40 mg/dl, a fasting triglyceride level of over 150 mg/dl or a history of use of lipid-lowering agents. The presence/absence of gallstones was determined by abdominal CT or ultrasonography. The presence/absence of gallstones of patients who had received cholecystectomy was determined by the previous record of abdominal CT or ultrasonography before cholecystectomy.

Table 1 Characteristics of subjects with or without ESEM

| | ESEM (+) cases (n = 528) | ESEM (-) controls (n = 528) |
|--|-----------------------------|--------------------------------|
| Age | | |
| Mean ± SD (years) | 65.3 ± 12.3 | 65.3 ± 12.3 |
| 20–29 | 6 (1.1%) | 6 (1.1%) |
| 30–39 | 16 (3.0%) | 16 (3.0%) |
| 40–49 | 34 (6.4%) | 34 (6.4%) |
| 50–59 | 91 (17.2%) | 91 (17.2%) |
| 60–69 | 148 (28.0%) | 148 (28.0%) |
| 70–79 | 189 (35.8%) | 189 (35.8%) |
| 80–89 | 44 (8.3%) | 44 (8.3%) |
| Gender | | |
| Male | 356 (67.4%) | 356 (67.4%) |
| Female | 172 (32.6%) | 172 (32.6%) |
| Hiatus hernia | | |
| Presence | 444 (84.1%) | 327 (61.9%) |
| Absence | 84 (15.9%) | 201 (38.1%) |
| Reflux esophagitis | | |
| None | 492 (93.2%) | 508 (96.2%) |
| Grade A | 16 (3.0%) | 11 (2.1%) |
| Grade B | 18 (3.4%) | 6 (1.1%) |
| Grade C | 1 (0.2%) | 3 (0.6%) |
| Grade D | 1 (0.2%) | 0 (0%) |
| Gastric mucosal atrophy | | |
| None | 104 (19.7%) | 104 (19.7%) |
| Mild | 228 (43.2%) | 268 (50.8%) |
| Moderate | 154 (29.2%) | 129 (24.4%) |
| Severe | 42 (8.0%) | 27 (5.1%) |
| Clinical background factors^a [no./total no. (%)] | | |
| Alcohol | 139/371 (37.5%) | 129/361 (35.7%) |
| Smoking | 171/374 (45.7%) | 158/367 (43.1%) |
| <i>H. pylori</i> | 105/149 (70.5%) | 83/112 (74.1%) |
| Obesity | 78/295 (26.4%) | 64/315 (20.3%) |
| BMI ± SD (kg/m ²) | 22.6 ± 4.0 | 22.4 ± 3.5 |
| Hypertension | 176/343 (51.3%) | 149/307 (48.5%) |
| Diabetes | 73/386 (18.9%) | 64/367 (17.4%) |
| Dyslipidemia | 120/210 (57.1%) | 120/201 (59.7%) |
| Gallstones | 85/371 (22.9%) | 64/392 (16.3%) |

ESEM endoscopically suspected esophageal metaplasia; BMI body mass index

^a Part of the information about the clinical background could not be collected from the subjects' medical records; therefore, total numbers of collected data for each factor were indicated in the clinical background section

Statistical analyses

The associations of endoscopic findings or clinical background factors with the presence of ESEM were evaluated by a logistic regression model with adjustment for age and gender. Trends of association of the severity of reflux

esophagitis and gastric mucosal atrophy with the presence of ESEM were evaluated by a logistic regression model that assigned scores to the level of the independent variable. The multivariate logistic regression model was conducted with adjustment for age, gender, hiatus hernia, reflux esophagitis, gastric mucosal atrophy, obesity and gallstones. All of the statistical analysis was performed using STATA 9.1 (Stata Corporation, College Station, TX). A two-sided *p* value of <0.05 was considered statistically significant.

Results

Association between endoscopic findings and ESEM

Among 528 subjects with ESEM, 64 subjects (12.1%) were diagnosed to have long segment ESEM, and 464 subjects (87.9%) were diagnosed to have short segment ESEM. According to the age- and gender-adjusted analysis, a strong association was detected between the presence of hiatus hernia and that of ESEM [odds ratio (OR) 3.40, 95% confidence interval (CI) 2.52–4.58]. The presence of grade B-D reflux esophagitis was significantly associated with the presence of ESEM (OR 2.31, 95% CI 1.04–5.14). Reflux esophagitis of greater severity grades was also significantly associated with the presence of ESEM (*p* = 0.02). In addition, gastric mucosal atrophy of greater severity grades was also significantly associated with the presence of ESEM (*p* = 0.04) (Table 2).

Association between clinical background factors and ESEM

All of the clinical background factors of the subjects could not be determined from the medical records. Therefore, the associations between the clinical background factors and the presence of ESEM were analyzed using partial subjects whose background could be determined. All of the determined rates of the background factors were not different between cases and controls. Among these background factors, only the presence of gallstones was significantly associated with that of ESEM (OR 1.56, 95% CI 1.09–2.25). The presence of obesity was possibly associated with that of ESEM (OR 1.43, 95% CI 0.98–2.10, *p* = 0.06) (Table 2).

Multivariate analysis for endoscopic findings, obesity, gallstones and ESEM

The age- and gender-adjusted analysis showed that the presence of hiatus hernia, gallstones and obesity, and the severity of reflux esophagitis and gastric mucosal atrophy

Table 2 Results for logistic regression analysis

| | ESEM (+) case no./total no. (%) | ESEM (-) control no./total no. (%) | Age- and gender-adjusted analysis | | Multivariate analysis ^a | |
|-------------------------|------------------------------------|---------------------------------------|-----------------------------------|----------------|------------------------------------|----------------|
| | | | Odds ratio (95% CI) | <i>p</i> value | Odds ratio (95% CI) | <i>p</i> value |
| Hiatus hernia | 444/528 (84.1%) | 327/528 (61.9%) | 3.40 (2.52–4.58)*** | <0.001 | 2.75 (1.75–4.33)*** | <0.001 |
| Reflux esophagitis | | | | | | |
| Grade A | 16/528 (3.0%) | 11/528 (2.1%) | 1.51 (0.69–3.29) | | 0.94 (0.27–3.22) | |
| Grade B–D | 20/528 (3.8%) | 9/528 (1.7%) | 2.31 (1.04–5.14)* | 0.02 (trend)* | 1.83 (0.51–6.61) | 0.43 (trend) |
| Gastric mucosal atrophy | | | | | | |
| Mild | 228/528 (43.2%) | 268/528 (50.8%) | 0.86 (0.62–1.19) | | 0.92 (0.56–1.51) | |
| Moderate | 154/528 (29.1%) | 129/528 (24.4%) | 1.22 (0.85–1.77) | | 1.56 (0.90–2.71) | |
| Severe | 42/528 (8.0%) | 27/528 (5.1%) | 1.60 (0.91–2.81) | 0.04 (trend)* | 1.67 (0.78–3.61) | 0.04 (trend)* |
| Alcohol | 139/371 (37.5%) | 129/361 (35.7%) | 1.04 (0.74–1.46) | 0.82 | | |
| Smoking | 171/374 (45.7%) | 158/367 (43.1%) | 1.09 (0.79–1.51) | 0.59 | | |
| <i>H. pylori</i> | 105/149 (70.5%) | 83/112 (74.1%) | 0.83 (0.48–1.45) | 0.52 | | |
| Obesity | 78/295 (26.4%) | 64/315 (20.3%) | 1.43 (0.98–2.10) [▲] | 0.06 | 1.20 (0.77–1.89) | 0.42 |
| Hypertension | 176/343 (51.3%) | 149/307 (48.5%) | 1.19 (0.86–1.64) | 0.30 | | |
| Diabetes | 73/386 (18.9%) | 64/367 (17.4%) | 1.11 (0.76–1.62) | 0.58 | | |
| Dyslipidemia | 120/210 (57.1%) | 120/201 (59.7%) | 0.97 (0.65–1.44) | 0.86 | | |
| Gallstones | 85/371 (22.9%) | 64/392 (16.3%) | 1.56 (1.09–2.25)* | 0.02 | 1.67 (1.03–2.69)* | 0.04 |

ESEM endoscopically suspected esophageal metaplasia; CI confidence interval

[▲] *p* < 0.1

* *p* < 0.05

*** *p* < 0.001

^a Adjustment for age, gender, hiatus hernia, reflux esophagitis, gastric mucosal atrophy, obesity and gallstones

were associated with ESEM. Therefore, the authors analyzed the association of these factors with the presence of ESEM by a multivariate logistic regression model (Table 2). The presence of hiatus hernia, gallstones and the severity of gastric mucosal atrophy were independently associated with the presence of ESEM.

Association of gastric mucosal atrophy and gallstones and ESEM

According to the Kimura–Takemoto classification, the presence of gastric corpus atrophy means moderate/severe gastric mucosal atrophy. The absence of gastric corpus atrophy means no/mild gastric mucosal atrophy. To assess the relationship among the presence of gastric corpus atrophy, gallstones and ESEM, the present subjects were re-allocated into four groups: subjects with neither gastric corpus atrophy nor gallstones, subjects with gastric corpus atrophy alone, subjects with gallstones alone, and subjects with both gastric corpus atrophy and gallstones. The associations of these four groups with the presence of ESEM were analyzed using a multivariate logistic regression model with adjustment for age, gender, hiatus hernia, reflux esophagitis, obesity and the three factors gastric

corpus atrophy alone, gallstones alone, and both gastric corpus atrophy and gallstones (Table 3).

Although the group with gallstones alone was not associated with the presence of ESEM (OR 1.59, 95% CI 0.87–2.92), the group with both gastric corpus atrophy and gallstones was strongly associated with the presence of ESEM (OR 2.94, 95% CI 1.40–6.17). The group with gastric corpus atrophy alone was also associated with the presence of ESEM (OR 1.63, 95% CI 1.03–2.57).

Discussion

The result of the present case control study showed that the presence of gallstones, hiatus hernia and the severity of gastric mucosal atrophy were independently associated with the presence of ESEM. It has been suggested that both gallstones and previous cholecystectomy contribute to the occurrence of duodeno-gastric reflux [16, 34–39]. The underlying mechanism is thought to be a dysfunction of the antroduodenal motor unit that favors the reflux of duodenal contents into the stomach [37]. According to the large population-based study, a moderately increased risk for esophageal adenocarcinoma following cholecystectomy

Table 3 Association of gastric mucosal atrophy and gallstones with ESEM

| | ESEM (+) cases No./total no. (%) | ESEM (-) controls No./total no. (%) | Odds ratio (95% CI) ^a | <i>p</i> value |
|---|-------------------------------------|--|----------------------------------|----------------|
| Factor 1: gastric corpus atrophy (+) ^b , gallstone (-) | 104/371 (28.0%) | 96/392 (24.5%) | 1.63 (1.03–2.57)* | 0.04 |
| Factor 2: gastric corpus atrophy (-) ^c , gallstone (+) | 45/371 (12.1%) | 44/392 (11.2%) | 1.59 (0.87–2.92) | 0.13 |
| Factor 3: gastric corpus atrophy (+) ^b , gallstone (+) | 40/371 (10.8%) | 20/392 (5.1%) | 2.94 (1.40–6.17)** | 0.004 |

ESEM endoscopically suspected esophageal metaplasia; CI confidence interval

* $p < 0.05$

** $p < 0.01$

^a Result of a multivariate logistic regression model with adjustment for age, gender, hiatus hernia, reflux esophagitis, obesity, factor 1, factor 2 and factor 3

^b The grade of gastric mucosal atrophy was moderate or severe

^c The grade of gastric mucosal atrophy was none or mild

was observed (OR 1.3, $p < 0.05$) [40]. In the present study, independent association of the presence of gallstones with that of ESEM was shown, suggesting that the duodeno-gastric bile reflux plays an important role in the development of ESEM, although the association of previous cholecystectomy with the presence of ESEM was not directly examined.

The present study also showed that the presence of hiatus hernia was associated with that of ESEM. Previous studies have shown a strong association of hiatus hernia with BE [41–43], suggesting the occurrence of gastro-esophageal reflux in hiatus hernia. On the other hand, the multivariate analysis revealed the severity of reflux esophagitis was not independently associated with the presence of ESEM. This result was consistent with that of the recent Korean study [24], which showed that 77.7% of BE patients did not have reflux esophagitis.

The association of the presence of *H. pylori* infection or the severity of gastric mucosal atrophy with the presence of ESEM was still controversial [41, 44, 45]. In general, many studies have shown that *H. pylori* infection and gastric mucosal atrophy are inversely associated with BE [25, 46]. However, the result of the present study suggested a positive association of the severity of gastric mucosal atrophy with the presence of ESEM, and the presence of *H. pylori* infection was not associated with the presence of ESEM. *H. pylori*-induced corpus atrophy reduces gastric acid secretion and the distal esophageal acid exposure [47], whereas gastric pH leads to bile precipitation in the stomach [48, 49]. Gastric acid would prevent gastro-esophageal bile reflux by precipitating bile, while gastric mucosal atrophy with low acid would accelerate the esophageal exposure of bile. In addition, duodeno-gastric bile reflux has been demonstrated to be associated with the development of intestinal metaplasia in the stomach as well as in the lower esophagus [50–52] (Fig. 2). Patients with BE have been shown to have bile-related gastritis [53, 54].

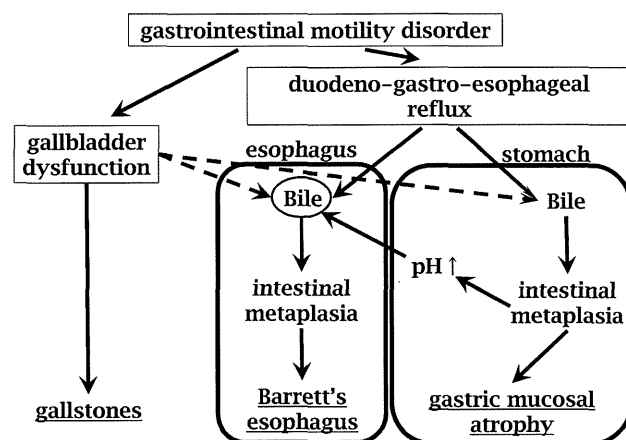


Fig. 2 The role of bile and gastric mucosal atrophy in the development of Barrett's esophagus. Bile might play a main role in the development of Barrett's esophagus. Lower esophageal bile exposure was caused by duodeno-gastro-esophageal reflux (DGER). Gallbladder dysfunction, which leads to the development of gallstones, is closely associated with the efficiency of continuous bile flow into the duodenum and the occurrence of DGER. This could be the reason why the presence of gallstones was associated with the presence of ESEM. On the other hand, DGER also caused gastric intestinal metaplasia and mucosal atrophy. In addition, gastric mucosal atrophy with low acid could enhance esophageal exposure to bile, which precipitates in the stomach with normal acidity

Table 3 shows that the presence of both gastric corpus atrophy and gallstones was associated with that of ESEM more strongly than the presence of gallstones alone, suggesting the acceleration of DGER by the combination with gastric corpus atrophy. In line with this, in a population of patients with a high prevalence of *H. pylori* infection like the Japanese population, gastric corpus atrophy may reflect an abnormal gastric exposure to bile and lead to an abnormal esophageal exposure to bile. Since most of the cases with ESEM in the present study had short segment ESEM, the disease of the present patients might be milder than that of the enrolled patients in the previous Western

studies. The positive association of gastric mucosal atrophy with ESEM suggests that the esophageal bile reflux is more important than acid reflux in the early stage of BE.

Although obesity is known to be associated with BE [55, 56], the multivariate analysis to investigate the association of gallstones and obesity with BE has not yet been reported. The result of the present study revealed that the presence of obesity was not an independent risk factor for ESEM, which means that the presence of obesity was confounding variable. Recent studies suggested that low plasma adiponectin is associated with the development of BE [26, 57]. On the other hand, low plasma adiponectin is thought to be also associated with the development of gallstones [58, 59]. In addition, obesity is known to increase the prevalence of hiatus hernia [60, 61]. Therefore, obesity may confound hiatus hernia or gallstones.

In conclusion, not only the presence of hiatus hernia, but also the presence of gallstones and the severity of gastric mucosal atrophy appear to be risk factors in the presence of ESEM in the Japanese outpatient population. The injurious potential of gallstones complications might be exacerbated by the presence of gastric corpus atrophy with low acid. These results suggest a causal association of distal esophageal bile exposure with the development of ESEM, which could be enhanced by severe gastric atrophy.

Acknowledgment This study was supported by Graduate School Doctoral Student Aid Program, Keio University (to J.M.), Grant-in-Aid for Exploratory Research from the Japan Society for the Promotion of Science (JSPS) (19659057, to H.S.) and Keio Gijyuku Academic Development Fund (to H.S.). The authors thank Prof. Nimish Vakil, University of Wisconsin Medical School, for his valuable instructions and suggestions for this report.

References

- Pera M, Cameron AJ, Trastek VF, Carpenter HA, Zinsmeister AR. Increasing incidence of adenocarcinoma of the esophagus and esophagogastric junction. *Gastroenterology*. 1993;104:510–3.
- Blot WJ, Devesa SS, Kneller RW, Fraumeni JF Jr. Rising incidence of adenocarcinoma of the esophagus and gastric cardia. *JAMA*. 1991;265:1287–9.
- Botterweck AA, Schouten LJ, Volovics A, Dorant E, van Den Brandt PA. Trends in incidence of adenocarcinoma of the oesophagus and gastric cardia in ten European countries. *Int J Epidemiol*. 2000;29:645–54.
- Eloubeidi MA, Mason AC, Desmond RA, El-Serag HB. Temporal trends (1973–1997) in survival of patients with esophageal adenocarcinoma in the United States: a glimmer of hope? *Am J Gastroenterol*. 2003;98:1627–33.
- Shaheen NJ, Sharma P, Overholt BF, Wolfsen HC, Sampliner RE, Wang KK, et al. Radiofrequency ablation in Barrett's esophagus with dysplasia. *N Engl J Med*. 2009;360:2277–88.
- Voutilainen M, Farkkila M, Juhola M, Nuorva K, Mauranen K, Mantynen T, et al. Specialized columnar epithelium of the esophagogastric junction: prevalence and associations. The Central Finland Endoscopy Study Group. *Am J Gastroenterol*. 1999;94:913–8.
- Vakil N, van Zanten SV, Kahrilas P, Dent J, Jones R. The Montreal definition and classification of gastroesophageal reflux disease: a global evidence-based consensus. *Am J Gastroenterol*. 2006;101:1900–20. quiz 1943.
- Richter JE. Importance of bile reflux in Barrett's esophagus. *Dig Dis*. 2000;18:208–16.
- Champion G, Richter JE, Vaezi MF, Singh S, Alexander R. Duodenogastroesophageal reflux: relationship to pH and importance in Barrett's esophagus. *Gastroenterology*. 1994;107:747–54.
- Nehra D, Howell P, Williams CP, Pye JK, Beynon J. Toxic bile acids in gastro-oesophageal reflux disease: influence of gastric acidity. *Gut*. 1999;44:598–602.
- Koek GH, Sifrim D, Lerut T, Janssens J, Tack J. Multivariate analysis of the association of acid and duodeno-gastro-oesophageal reflux exposure with the presence of oesophagitis, the severity of oesophagitis and Barrett's oesophagus. *Gut*. 2008;57:1056–64.
- Izbeki F, Rosztozy AI, Yobuta JS, Roka R, Lonovics J, Wittmann T. Increased prevalence of gallstone disease and impaired gallbladder motility in patients with Barrett's esophagus. *Dig Dis Sci*. 2008;53:2268–75.
- Johnston DE, Kaplan MM. Pathogenesis and treatment of gallstones. *N Engl J Med*. 1993;328:412–21.
- Shih WJ, Coupal JJ, Domstad PA, Ram MD, DeLand FH. Disorders of gallbladder function related to duodenogastric reflux in technetium-99 m DISIDA hepatobiliary scintigraphy. *Clin Nucl Med*. 1987;12:857–60.
- Kennedy NS, Campbell FC, Cullen PT, Sutton DG, Millar BW, Cuschieri A. Gallbladder function and fasting enterogastric bile reflux. *Nucl Med Commun*. 1989;10:193–8.
- Svensson JO, Gelin J, Svanvik J. Gallstones, cholecystectomy, and duodenogastric reflux of bile acid. *Scand J Gastroenterol*. 1986;21:181–7.
- Hongo M. Review article: Barrett's oesophagus and carcinoma in Japan. *Aliment Pharmacol Ther*. 2004;20(Suppl 8):50–4.
- Hongo M, Shoji T. Epidemiology of reflux disease and CLE in East Asia. *J Gastroenterol*. 2003;38(Suppl 15):25–30.
- Wang KK, Sampliner RE. Updated guidelines 2008 for the diagnosis, surveillance and therapy of Barrett's esophagus. *Am J Gastroenterol*. 2008;103:788–97.
- Jones TF, Sharma P, Daaboul B, Cherian R, Mayo M, Topalovski M, et al. Yield of intestinal metaplasia in patients with suspected short-segment Barrett's esophagus (SSBE) on repeat endoscopy. *Dig Dis Sci*. 2002;47:2108–11.
- Kim GH, Song GA, Kim TO, Jo HJ, Kim do H, Heo J, et al. Endoscopic grading of gastroesophageal flap valve and atrophic gastritis is helpful to predict gastroesophageal reflux. *J Gastroenterol Hepatol*. 2008;23:208–14.
- Ford AC, Forman D, Reynolds PD, Cooper BT, Moayyedi P. Ethnicity, gender, and socioeconomic status as risk factors for esophagitis and Barrett's esophagus. *Am J Epidemiol*. 2005;162:454–60.
- Edelstein ZR, Bronner MP, Rosen SN, Vaughan TL. Risk factors for Barrett's esophagus among patients with gastroesophageal reflux disease: a community clinic-based case-control study. *Am J Gastroenterol*. 2009;104:834–42.
- Park JJ, Kim JW, Kim HJ, Chung MG, Park SM, Baik GH, et al. The prevalence of and risk factors for Barrett esophagus in a Korean population: A Nationwide Multicenter Prospective Study. *J Clin Gastroenterol*. 2009 (Epub ahead of print).
- Anandasabapathy S, Jhamb J, Davila M, Wei C, Morris J, Bresalier R. Clinical and endoscopic factors predict higher pathologic grades of Barrett dysplasia. *Cancer*. 2007;109:668–74.
- Rubenstein JH, Dahlkemper A, Kao JY, Zhang M, Morgenstern H, McMahon L, et al. A pilot study of the association of low

- plasma adiponectin and Barrett's esophagus. *Am J Gastroenterol*. 2008;103:1358–64.
27. Avidan B, Sonnenberg A, Schnell TG, Chejfec G, Metz A, Sontag SJ. Hiatal hernia size, Barrett's length, and severity of acid reflux are all risk factors for esophageal adenocarcinoma. *Am J Gastroenterol*. 2002;97:1930–6.
 28. Sharma P, Dent J, Armstrong D, Bergman JJ, Gossner L, Hoshihara Y, et al. The development and validation of an endoscopic grading system for Barrett's esophagus: the Prague C & M criteria. *Gastroenterology*. 2006;131:1392–9.
 29. Vianna A, Hayes PC, Moscoso G, Driver M, Portmann B, Westaby D, et al. Normal venous circulation of the gastroesophageal junction. A route to understanding varices. *Gastroenterology*. 1987;93:87–89.
 30. Kimura K, Satoh K, Ido K, Taniguchi Y, Takimoto T, Takemoto T. Gastritis in the Japanese stomach. *Scand J Gastroenterol Suppl*. 1996;214:17–20. discussion 21–13.
 31. Kimura K, Takemoto T. An endoscopic recognition of the atrophic border and its significance in chronic gastritis. *Endoscopy*. 1969;3:87–97.
 32. Ismail T, Bancewicz J, Barlow J. Endoscopic appearance of the gastroesophageal valve and competence of the cardia. *Diagn Ther Endosc*. 1996;2:147–50.
 33. Lundell LR, Dent J, Bennett JR, Blum AL, Armstrong D, Galmiche JP, et al. Endoscopic assessment of oesophagitis: clinical and functional correlates and further validation of the Los Angeles classification. *Gut*. 1999;45:172–80.
 34. Brough WA, Taylor TV, Torrance HB. The surgical factors influencing duodenogastric reflux. *Br J Surg*. 1984;71:770–3.
 35. Johnson AG. Pyloric function and gall-stone dyspepsia. *Br J Surg*. 1972;59:449–54.
 36. Cabrol J, Navarro X, Simo-Deu J, Segura R. Evaluation of duodenogastric reflux in gallstone disease before and after simple cholecystectomy. *Am J Surg*. 1990;160:283–6.
 37. Perdakis G, Wilson P, Hinder R, Redmond E, Wetscher G, Neary P, et al. Altered antroduodenal motility after cholecystectomy. *Am J Surg*. 1994;168:609–14. discussion 614–605.
 38. Lorusso D, Misciagna G, Mangini V, Messa C, Cavallini A, Caruso ML, et al. Duodenogastric reflux of bile acids, gastrin and parietal cells, and gastric acid secretion before and 6 months after cholecystectomy. *Am J Surg*. 1990;159:575–8.
 39. Fein M, Bueter M, Sailer M, Fuchs KH. Effect of cholecystectomy on gastric and esophageal bile reflux in patients with upper gastrointestinal symptoms. *Dig Dis Sci*. 2008;53:1186–91.
 40. Freedman J, Ye W, Naslund E, Lagergren J. Association between cholecystectomy and adenocarcinoma of the esophagus. *Gastroenterology*. 2001;121:548–53.
 41. Okita K, Amano Y, Takahashi Y, Mishima Y, Moriyama N, Ishimura N, et al. Barrett's esophagus in Japanese patients: its prevalence, form, and elongation. *J Gastroenterol*. 2008;43:928–34.
 42. Cameron AJ. Barrett's esophagus: prevalence and size of hiatal hernia. *Am J Gastroenterol*. 1999;94:2054–9.
 43. Weston AP, Sharma P, Mathur S, Banerjee S, Jafri AK, Cherian R, et al. Risk stratification of Barrett's esophagus: updated prospective multivariate analysis. *Am J Gastroenterol*. 2004;99:1657–66.
 44. Fujiwara Y, Higuchi K, Shiba M, Watanabe T, Tominaga K, Oshitani N, et al. Association between gastroesophageal flap valve, reflux esophagitis, Barrett's epithelium, and atrophic gastritis assessed by endoscopy in Japanese patients. *J Gastroenterol*. 2003;38:533–9.
 45. Moriichi K, Watari J, Das KM, Tanabe H, Fujiya M, Ashida T, et al. Effects of *Helicobacter pylori* infection on genetic instability, the aberrant CpG island methylation status and the cellular phenotype in Barrett's esophagus in a Japanese population. *Int J Cancer*. 2009;124:1263–9.
 46. Anderson LA, Murphy SJ, Johnston BT, Watson RG, Ferguson HR, Bamford KB, et al. Relationship between *Helicobacter pylori* infection and gastric atrophy and the stages of the oesophageal inflammation, metaplasia, adenocarcinoma sequence: results from the FINBAR case-control study. *Gut*. 2008;57:734–9.
 47. Suzuki H, Hibi T, Marshall BJ. *Helicobacter pylori*: present status and future prospects in Japan. *J Gastroenterol*. 2007;42:1–15.
 48. Hofmann AF, Mysels KJ. Bile acid solubility and precipitation in vitro and in vivo: the role of conjugation, pH, and Ca²⁺ ions. *J Lipid Res*. 1992;33:617–26.
 49. Zentler-Munro PL, Fine DR, Batten JC, Northfield TC. Effect of cimetidine on enzyme inactivation, bile acid precipitation, and lipid solubilisation in pancreatic steatorrhoea due to cystic fibrosis. *Gut*. 1985;26:892–901.
 50. Masci E, Testoni PA, Fanti L, Guslandi M, Zuin M, Tittobello A. Duodenogastric reflux: correlations among bile acid pattern, mucus secretion, and mucosal damage. *Scand J Gastroenterol*. 1987;22:308–12.
 51. Bechi P, Amorosi A, Mazzanti R, Dei R, Bianchi S, Mugnai L, et al. Reflux-related gastric mucosal injury is associated with increased mucosal histamine content in humans. *Gastroenterology*. 1993;104:1057–63.
 52. Sobala GM, O'Connor HJ, Dewar EP, King RF, Axon AT, Dixon MF. Bile reflux and intestinal metaplasia in gastric mucosa. *J Clin Pathol*. 1993;46:235–40.
 53. Dixon MF, Neville PM, Mapstone NP, Moayyedi P, Axon AT. Bile reflux gastritis and Barrett's oesophagus: further evidence of a role for duodenogastro-oesophageal reflux? *Gut*. 2001;49:359–63.
 54. Mason RJ, Bremner CG. Gastritis in Barrett's esophagus. *World J Surg*. 1995;19:96–100. discussion 100–101.
 55. Wong A, Fitzgerald RC. Epidemiologic risk factors for Barrett's esophagus and associated adenocarcinoma. *Clin Gastroenterol Hepatol*. 2005;3:1–10.
 56. Wood RK, Yang YX. Barrett's esophagus in 2008: an update. *Keio J Med*. 2008;57:132–8.
 57. Iwasaki E, Suzuki H, Sugino Y, Iida T, Nishizawa T, Masaoka T, et al. Decreased levels of adiponectin in obese patients with gastroesophageal reflux evaluated by videoesophagography: possible relationship between gastroesophageal reflux and metabolic syndrome. *J Gastroenterol Hepatol*. 2008;23(Suppl 2):S216–21.
 58. Wang SN, Yeh YT, Yu ML, Dai CY, Chi WC, Chung WL, et al. Hyperleptinaemia and hypo adiponectinaemia are associated with gallstone disease. *Eur J Clin Invest*. 2006;36:176–80.
 59. Wang SN, Yeh YT, Yu ML, Wang CL, Lee KT. Serum adiponectin levels in cholesterol and pigment cholelithiasis. *Br J Surg*. 2006;93:981–6.
 60. Friedenberg FK, Xanthopoulos M, Foster GD, Richter JE. The association between gastroesophageal reflux disease and obesity. *Am J Gastroenterol*. 2008;103:2111–22.
 61. de Vries DR, van Herwaarden MA, Smout AJ, Samsom M. Gastroesophageal pressure gradients in gastroesophageal reflux disease: relations with hiatal hernia, body mass index, and esophageal acid exposure. *Am J Gastroenterol*. 2008;103:1349–54.

Delayed gastric emptying and disruption of the interstitial cells of Cajal network after gastric ischaemia and reperfusion

S. SUZUKI,*,†, H. SUZUKI,*, K. HORIGUCHI,‡, H. TSUGAWA,*, J. MATSUZAKI,*, T. TAKAGI,§, N. SHIMOJIMA¶ & T. HIBI*

*Division of Gastroenterology and Hepatology, Department of Internal Medicine, Keio University School of Medicine, Tokyo, Japan

†TSUMURA Research Laboratories, TSUMURA & Co., Ibaraki, Japan

‡Department of Anatomy, Faculty of Medical Sciences, University of Fukui, Fukui, Japan

§Molecular Gastroenterology and Hepatology, Graduate School of Medical Science, Kyoto Prefectural University of Medicine, Kyoto, Japan

¶Division of Pediatric Surgery, Department of Surgery, Keio University School of Medicine, Tokyo, Japan

Abstract

Background Gastrointestinal tract is one of the most susceptible organ systems to ischaemia. Not only mucosal injury but also alterations of the intestinal motility and loss of interstitial cells of Cajal (ICC) have been reported in response to ischaemia and reperfusion (I/R). However, there are few reports on the changes in the gastric motility after gastric I/R. The present study was designed to investigate the alterations in gastric emptying, the ICC and enteric nerves that regulate smooth muscle function in response to gastric I/R. **Methods** Seven-week-old male Wistar rats were exposed to gastric I/R, and the gastric emptying rates at 12 and 48 h after I/R were evaluated by the phenol red method. Expressions of gene product of *c-kit* receptor tyrosine kinase (*c-Kit*), a marker of ICC, and of neuronal proteins were also examined. **Key Results** Gastric emptying was transiently delayed at 12 h after I/R, but returned to normal by 48 h. Expression of *c-Kit* protein as assessed by Western blotting and immunofluorescent staining of the smooth muscle layer, as well as expression of the mRNA of stem cell factor, the ligand for *c-Kit*, were reduced at both 12 and 48 h after I/R. The expression

of neuronal nitric oxide synthase (*nNOS*) protein as assessed by Western blotting and immunofluorescent staining was also decreased at 12 h after I/R, but was restored to normal by 48 h. **Conclusions & Inferences** Gastric I/R evokes transient gastroparesis with delayed gastric emptying, associated with disruption of the ICC network and *nNOS*-positive neurons.

Keywords gastric emptying, gastric ischaemia and reperfusion, gastroparesis, interstitial cells of Cajal, neuronal nitric oxide synthase.

Abbreviations: ChAT, choline acetyltransferase; *c-Kit*, gene product of *c-kit* receptor tyrosine kinase; GAPDH, glyceraldehyde-3-phosphate; ICC, the interstitial cells of Cajal; ICC-IM, intramuscular interstitial cells of Cajal; ICC-MY, myenteric interstitial cells of Cajal; I/R, ischaemia and reperfusion; *nNOS*, neuronal nitric oxide synthase; NOD, non-obese diabetic; SCF, stem cell factor; TUNEL, terminal deoxynucleotidyl transferase-mediated dUTP nick end labelling.

INTRODUCTION

Gastrointestinal tract is one of the most susceptible organ systems to ischaemia. Previous investigations have demonstrated that ischaemia and reperfusion (I/R) is a major contributor to gastric mucosal injury caused by stress, such as burn stress¹ or haemorrhagic shock,² non-steroidal anti-inflammatory drugs³ and *Helicobacter pylori* infection.^{4,5} In an intestinal I/R model, not only post-ischaemic mucosal injury but also the alterations of the intestinal motility have been reported.^{6–8} However, there are few reports on the alterations of gastric motility after gastric I/R.

Address for correspondence

Hidekazu Suzuki MD, PhD, Division of Gastroenterology and Hepatology, Department of Internal Medicine, Keio University School of Medicine, 35 Shinanomachi, Shinjuku-ku, Tokyo 160-8582, Japan.

Tel: +81 3 5363 3914; fax: 81 3 5363 3967;

e-mail: hsuzuki@sc.itc.keio.ac.jp

Received: 16 July 2009

Accepted for publication: 13 November 2009

Disruption of the network of interstitial cells of Cajal (ICC) has been reported along with intestinal dysmotility after intestinal I/R.⁸ However, the precise effect of gastric I/R on the gastric ICC network is not yet clear. The interstitial cells of Cajal, which express the proto-oncogene *c-kit* receptor tyrosine kinase (gene product, c-Kit), play critical roles in gastrointestinal motility.^{9,10} c-Kit is essential for the development of the ICC and maintenance of their phenotype,^{11,12} and the natural ligand for c-Kit is stem cell factor (SCF). Two classes of ICC have been identified in the mammalian stomach: myenteric ICC (ICC-MY), which lie in the space between the circular and longitudinal muscles in the region around the myenteric plexus and have been identified as the source of the electrical slow waves underlying the phasic contractions of the gastric musculature,¹³ and intramuscular ICC (ICC-IM), which are found in the circular and longitudinal muscle layers and mediate excitatory and inhibitory inputs to the musculature from the enteric motor neurons.^{14,15}

The interstitial cells of Cajal and enteric nerves are often found in proximity and their interactions seem to be required for normal functioning of the gastrointestinal tract. In nearly all human motility disorders associated with the loss of the ICC, there is also a concomitant loss of enteric neurons. When the subtypes of enteric neurons that are lost in association with ICC loss were examined, a decrease in the neuronal nitric oxide synthase (nNOS) expression was also revealed.^{16–20} nNOS is expressed in the neurons of the myenteric plexus in the gastrointestinal tract. Nitric oxide released by the activation of nNOS functions as a major inhibitory non-adrenergic, non-cholinergic neurotransmitter that is involved in reflex relaxation of the gastric fundus to accommodate food or fluid, and mediates pyloric relaxation and intestinal feedback regulation, thereby facilitating gastric emptying.²¹ As delayed gastric emptying has been noted following treatment with 7-nitroindazole, an nNOS-selective inhibitor²² and in nNOS-knockout mice,²³ nNOS is considered to play an important role in gastric emptying.

The present study was designed to investigate the alterations in gastric motility, the ICC and the enteric nerves that regulate smooth muscle function in a rat model of gastric I/R injury.

MATERIALS AND METHODS

Ischaemia and reperfusion

Six-week-old male Wistar rats were purchased from Japan SLC Inc. (Shizuoka, Japan). All rats were handled according to the

guidelines of the Keio University Animal Research Committee. All rats were used after acclimatization for 1 week and denied access to food for 22–24 h (free access to water) before the operation and kept starved until sacrifice. When reperfusion was established for 48 h, the rats were fed after the operation, but denied access to food for 24 h before the sacrifice. The rats were anaesthetized with sodium pentobarbital (50 mg kg⁻¹, i.p.) during the experiments. The abdomen was opened by a midline incision and the celiac artery was occluded with a small clamp for 80 min. Reperfusion was established for 12 or 48 h by removal of the clamp. Gastric mucosal injury was confirmed by haematoxylin–eosin staining in all the rats exposed to gastric I/R. For comparison, some rats were subjected to sham operation (surgery, but no clamping).

Evaluation of gastric emptying

The experiment was conducted according to the method reported by Kido *et al.*²⁴ One millilitre of phenol red (100 µg mL⁻¹) was administered orally to the rats, which were then sacrificed 15 min after the administration, except for those animals that were sacrificed immediately after the injection to recover the entire dose of phenol red. The stomach was removed immediately and washed in 10 mL of Na₂HPO₄ solution (0.1 mol L⁻¹) to collect the gastric contents and phenol red, and then 1 mL of rinse solution was added to 0.5 mL of Na₂HPO₄ solution (0.1 mol L⁻¹) (S1). The residual rinse solution was added to 1 mL of phenol red (100 µg mL⁻¹) solution and diluted fivefold with Na₂HPO₄ solution (0.1 mol L⁻¹) (S2). The absorbances of the S1 and S2 solutions were measured at a wavelength of 570 nm with a microplate reader (BIO-RAD, Hercules, CA, USA). Gastric emptying was calculated as follows:

$$\text{Gastric emptying(\%)} = 100 - (A/B) \times 100$$

A: Residual amount of phenol red in the stomach (µg)

$$= (100 - (1.5 \times \langle S1 \rangle)) / (5 \times \langle S2 \rangle / (1.5 \times \langle S1 \rangle) - 1)$$

Note: <S1> and <S2> denote the phenol red concentrations in the S1 and S2 solutions.

B: Amount of phenol red recovered from the stomach immediately after the phenol red administration (µg).

Preparation of total RNA and quantitative RT-PCR analysis

Total RNA was extracted from the total stomach tissue using RNeasy Mini kit (Qiagen, Valencia, CA, USA), and DNase treatment was performed with an RNase-free DNase set (Qiagen). RNA was converted into cDNA using the PrimeScript RT reagent kit (Takara, Ohtsu, Japan). Quantitative RT-PCR analysis was performed using Dice (Takara) with SYBR Premix Ex TaqII (Takara). The primer sequences used were as follows – *c-kit* mRNA: 5'-ATC CAG CCC CAC ACC CTG TT-3' and 5'-TGT AGG CAA GAA CCA TCA CAA TGA-3', SCF (membrane-bound isoform) mRNA: 5'-TGA GAA AGG GAA AGC CGC-3' and 5'-TAA GGC TCC AAA AGC AAA GC-3', choline acetyltransferase (ChAT) mRNA: 5'-CAA CCA TCT TCT GGC ACT GA-3' and 5'-TAG CAG GCT CCA TAG CCA TT-3', nNOS mRNA: 5'-TCA AAG CCA TCC AGC GCA TA-3', 5'-GCG GTT GGT CAC TTC ATA CGT TC-3', glyceraldehyde-3-phosphate (GAPDH) mRNA: 5'-GGC ACA GTC AAG GCT GAG AAT G-3', 5'-ATG GTG GTG AAG ACG CCA GTA-3'. The mRNA expression levels were normalized using the GAPDH mRNA expression levels.

Western blot analysis

Liquid nitrogen-frozen specimens of the total stomach were homogenized in ice-cold RIPA Buffer (Upstate, Temecula, CA, USA) containing protease inhibitor cocktail (Sigma Chemical Co., St Louis, MO, USA), incubated on ice for 30 min, centrifuged at 10 000 g for 15 min, and the supernatants were used as the total proteins. The total protein concentration was measured with the BCA™ Protein Assay kit (PIERCE, Rockford, IL, USA). Total proteins were separated by 12% NuPAGE Bis-Tris gel (Invitrogen, Carlsbad, CA, USA) electrophoresis and transferred to polyvinylidene difluoride membranes (Invitrogen). The blots were blocked with Block Ace (Dainippon Sumitomo Pharma Co., Osaka, Japan) and probed with anti-nNOS antibody (1 : 5000; ZYMED, San Francisco, CA, USA), anti-c-Kit antibody (1 : 5000, sc-1494; Santa Cruz Biotechnologies, Heidelberg, Germany) or anti-ChAT antibody (1 : 1000; Abcam, Cambridge, UK), followed by reprobing with anti- β -actin antibody (1 : 20 000, clone: AC-74, SIGMA) as the loading control. Signal detection of the immunoreactive bands was facilitated by enhanced chemiluminescence using ECL plus (GE Healthcare, Uppsala, Sweden). Band quantification was performed using the IMAGEJ program (National Institutes of Health, Bethesda, MD, USA).

Immunofluorescent staining

For immunofluorescent staining of c-Kit, stomach tissue specimens were fixed with 2% periodate-lysine paraformaldehyde for 6 h and embedded in Tissue-Tek OCT compound 4583 (Sakura Finetechnical Co. Ltd. Tokyo, Japan), frozen in liquid isopentane cooled with liquid nitrogen and cut into 5- μ m sections with a cryostat (CM1850, Leica, Nussloch, Germany). The sections were placed on a micro slide glass (Matsunami, Osaka, Japan) and incubated with Protein Block (DAKO Japan, Tokyo, Japan) containing 0.5% Triton X-100 for 1 h at room temperature and incubated with goat anti-c-Kit polyclonal antibody (sc-1494; 1 : 200, Santa Cruz Biotechnology) overnight at 4 °C. Immunoreactivity was detected using Alexa Fluor 488 donkey anti-goat IgG (1 : 1000, Molecular Probes, Eugene, OR, USA). Coverslips were mounted with Permafluor (Beckman Coulter, Fullerton, CA, USA) and immunofluorescence was examined using a Nikon Eclipse E600 microscope (Nikon Corporation, Tokyo, Japan).

For immunofluorescent staining of nNOS, stomach tissue specimens were fixed in 10% neutralized formalin and embedded in paraffin. After deparaffinization and hydration, the antigens were retrieved by heating for 20 min at 97 °C in citrate buffer (10 mmol L⁻¹, pH 6.0). Nonspecific binding was blocked by Protein Block (DAKO Japan). Sections were incubated overnight at 4 °C with anti-nNOS antibody (1 : 100, ZYMED). Immunoreactivity was detected using Alexa Fluor 568 goat anti-rabbit IgG (Molecular Probes). The areas of the c-Kit- and nNOS-positive cells were quantified using the IMAGEJ program (National Institutes of Health) and normalized by the areas of the smooth muscle layers.

For whole-mount immunofluorescent staining, the stomach was opened along the greater curvature, pinned to a dish filled with Sylgard elastomer (Dow Corning Corp., Midland, MI, USA) and stretched to 150% of the resting length before being fixed with ice-cold acetone for 30 min. The mucosa was removed by sharp dissection. After being washed with PBS containing 0.3% Triton X-100 for 10 min at 4 °C, the musculature was incubated in normal donkey serum (5% in PBS containing 2% bovine serum albumin and 0.2% sodium azide) for 20 min at 4 °C. Tissues were incubated with goat anti-c-Kit polyclonal antibody (sc-1494; 1 : 200; Santa Cruz Biotechnology, Inc.) and rabbit anti-PGP9.5

antibody (1 : 5000; Ultraclone, Cambridge, UK) or anti-nNOS antibody (1 : 100; ZYMED) and mouse monoclonal PGP9.5 antibody (1 : 30; Abcam) diluted in PBS containing 2% bovine serum albumin and 0.2% sodium azide overnight at 4 °C. Immunoreactivity was detected using Alexa Fluor 488 anti-goat IgG, Alexa Fluor 568 anti-rabbit IgG and Alexa Fluor 488 anti-mouse IgG (Molecular Probes) and visualized using a Leica TCS SP5 system (Leica) with adequate filter cubes. For the nerve counts, a total of 10 myenteric ganglia was analysed in each preparation ($n = 3$). PGP9.5 was used as a general neuronal marker to ascertain the total number of cell bodies, and the nNOS neuron population was expressed relative to the number of PGP9.5-positive neurons. PGP9.5 immunoreactivity was expressed by the number of PGP9.5-positive neurons normalized by the area of each ganglion.

Electron microscopy

Whole stomach specimens of I/R or sham-operated rats were opened and pinned as mentioned above. The tissue specimens were then placed in a fixative containing 3% glutaraldehyde and 4% paraformaldehyde in 0.1 mol L⁻¹ phosphate buffer, pH 7.4, overnight at room temperature. Following fixation, the tissue specimens were cut into small pieces and placed in the same buffer. Then, the tissues were post-fixed in 1% osmium tetroxide for 2 h at 4 °C. After being rinsed in distilled water, the tissues were stained en bloc with 3% aqueous uranyl acetate overnight, dehydrated in a graded series of ethyl alcohol and embedded in Epon epoxy resin. Ultrathin sections were cut using a Reichert microtome and double-stained with uranyl acetate and lead citrate before viewing under a Hitachi H7000 electron microscope (Hitachi, Ltd., Tokyo, Japan).

Statistical analysis

All values were expressed as mean \pm SD. The statistical significance of any differences between two groups was evaluated using unpaired Student's *t*-test. Statistical significance was accepted at $P < 0.05$, unless otherwise indicated.

RESULTS

Liquid gastric emptying

Liquid gastric emptying rates in the sham-operated rats and I/R rats were evaluated using the phenol red method. Although, the gastric emptying rates were significantly delayed at 12 h after I/R as compared with those in the sham-operated rats (sham: 55.5 \pm 11.9%; I/R: 43.0 \pm 11.8%; $P < 0.01$), the rates were normalized by 48 h after the I/R (Fig. 1).

c-Kit and membrane-bound SCF expression

The expression of *c-kit* and membrane-bound SCF mRNA was assessed by quantitative RT-PCR analysis. In Fig. 2A,B, significant decrease of the expression of *c-kit* mRNA (29.1 \pm 5.44% at 12 h and 56.4 \pm 35.0% at 48 h after I/R as compared with sham) and SCF mRNA (49.9 \pm 16.3% at 12 h and 69.1 \pm 16.7% at 48 h after I/

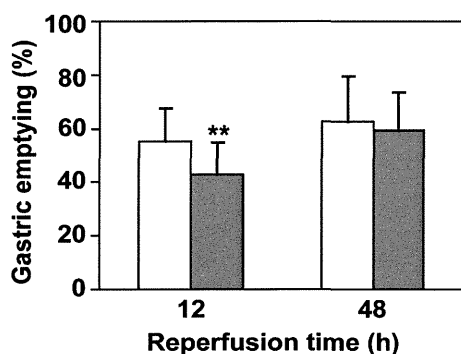


Figure 1 Liquid gastric emptying rates of sham-operated rats (open bar) and I/R rats (filled bar) at 12 h (Sham; $n = 18$, I/R; $n = 17$) and 48 h (Sham; $n = 12$, I/R; $n = 13$) after I/R. Data are means \pm SD. ** $P < 0.01$ as compared with sham-operated rats.

R as compared with sham) was observed at 12 and 48 h after I/R as compared with that in the stomach of the sham-operated rats. Western blot analysis also revealed significantly reduced expression of the c-Kit protein (approximately 145 kDa) at 12 and 48 h after I/R (Fig. 2C,D: $40.2 \pm 12.5\%$ at 12 h and $40.3 \pm 12.5\%$ at 48 h after I/R as compared with the observation in the sham group).

Immunofluorescent staining for c-Kit after I/R

Cross-sectional analysis along the long axis of the stomach was performed using anti-c-Kit antibody (Fig. 3A). Fluorescent immunostaining showed punctate staining in the circular muscle (ICC-IM) and a

layered signal in the myenteric plexus (ICC-MY). At 12 h after I/R, significant decrease of both ICC-IM and ICC-MY was observed in the corpus ($59.4 \pm 14.3\%$ and $66.0 \pm 24.6\%$ relative to the value in the sham group), while significant decrease of only ICC-IM was noted in the antrum ($50.1 \pm 20.7\%$ relative to the value in the sham group) in Fig. 3B. At 48 h after I/R, the areas of the c-Kit-positive cells were restored in the corpus, but remained reduced in the antrum. At 48 h after I/R, significant reduction not only of ICC-IM but also of ICC-MY was observed in the antrum as compared with the observation in the sham group, as shown in Fig. 3B ($71.5 \pm 21.7\%$ and $52.5 \pm 27.5\%$ relative to the value in the sham group).

Whole-mount staining was also performed using anti-c-Kit antibody and anti-PGP9.5 antibody. Fig. 3C shows overlays of optical sections representing the myenteric region. In the specimens from the sham-operated rats, dense networks of c-Kit-positive cells were observed. However, such networks were scarcely seen in the corpus of the I/R rats at 12 h. In the antrum, slight decrease of the ICC density was observed in the I/R rat, although the difference was not prominent as compared with that in the corpus.

nNOS and ChAT expression

In Fig. 4A, significant decrease of the nNOS mRNA at 12 h after I/R was observed ($29.4 \pm 4.97\%$) as compared with that in the stomach of the sham-operated rats, but the levels were restored at 48 h after I/R. The

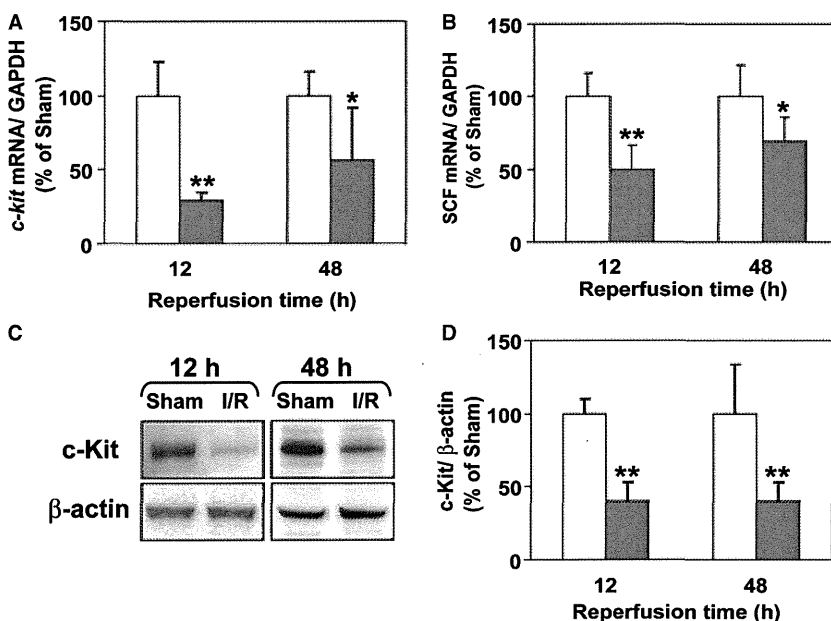


Figure 2 Expression levels of *c-kit* and SCF in the stomach of sham-operated rats (open bar) and I/R rats (filled bar) at 12 h (Sham; $n = 6$, I/R; $n = 7$) and 48 h (Sham; $n = 6$, I/R; $n = 7$) after I/R. Expression of *c-kit* (A) and SCF (B) mRNA as assessed by quantitative RT-PCR. (C) Western blot analysis of c-Kit. (D) Band quantification was performed using the IMAGEJ program. Data are means \pm SD. * $P < 0.05$ and ** $P < 0.01$ as compared with sham-operated rats.

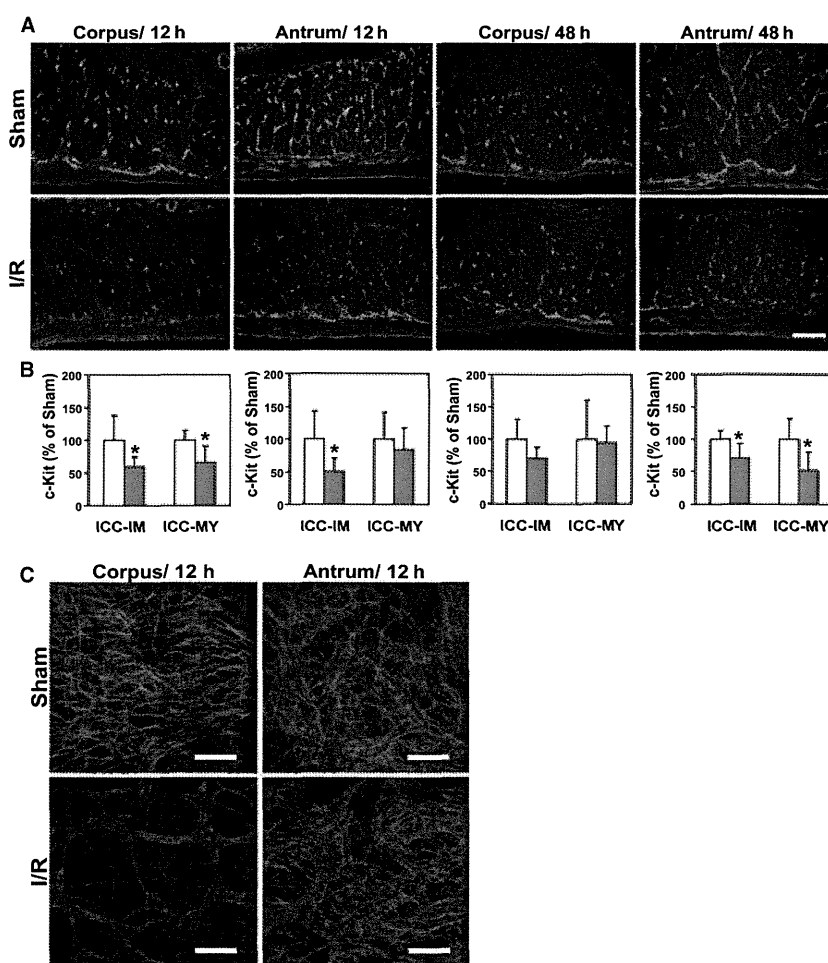


Figure 3 (A) Representative immuno-fluorescent staining for c-Kit in the corpus and antrum of a sham-operated rat and an I/R rat at 12 and 48 h after I/R. Bar, 100 μ m. (B) Areas of ICC-IM and ICC-MY were quantified using the image analysis software and are shown below the fluorescent images [Sham (open bar); $n = 6$, I/R (filled bar); $n = 7$]. Data are means \pm SD. * $P < 0.05$ as compared with sham-operated rats. (C) Representative images of whole-mount immunofluorescent staining for c-Kit (green) and PGP9.5 (red) in the corpus and antrum in a sham-operated rat and an I/R rat at 12 h after I/R. Bar, 150 μ m.

expression level of ChAT mRNA was not significantly different as compared with that in the sham-operated rats at both 12 h and at 48 h after I/R (Fig. 4B).

Western blot analysis showed reduced expression of the gastric nNOS proteins (upper band, approximately 155 kDa) at 12 h after I/R ($67.8 \pm 11.2\%$ relative to the value of sham-operated rats), but the expression levels at 48 h were the same as those in the specimens from the sham-operated rats (Fig. 4C). However, no changes in expression of the ChAT proteins (approximately 70 kDa) were observed throughout the experimental period (Fig. 4D).

Immunofluorescent staining for nNOS after I/R

Cross-sectional analysis along the long axis of the stomach was performed using anti-nNOS antibody (Fig. 5A). Fluorescent immunostaining of the corpus, antrum and pyloric sphincter muscle sections showed significantly decreased nNOS-positive areas in the

specimens at 12 h after I/R as compared with the value in the sham-operated rats, as shown in Fig. 5B ($63.0 \pm 30.0\%$, $56.8 \pm 13.7\%$ and $62.4 \pm 19.2\%$, respectively, as compared with the values in the sham group). However, the nNOS-immunoreactivities at 48 h after I/R were the same as those in the specimens from the sham-operated rats (data not shown).

Representative pictures of whole-mount staining of nNOS and PGP9.5 are shown in Fig. 5C. Slight but significant decrease in the count of PGP9.5-immunoreactive cells was observed in the corpus of the I/R rats ($81.4 \pm 2.15\%$ of the value in the sham-operated rats) as compared with that in the sham-operated rats, while no significant difference was noted in the antrum (Fig. 5D). The population of nNOS-positive neurons was $25.6 \pm 1.14\%$ in the corpus and $28.7 \pm 1.95\%$ in the antrum of the sham-operated rats. However, significant decrease in the population of nNOS-positive neurons at 12 h was observed in both the corpus ($12.4 \pm 4.42\%$) and antrum ($15.6 \pm 0.65\%$) in the I/R rats (Fig. 5E).

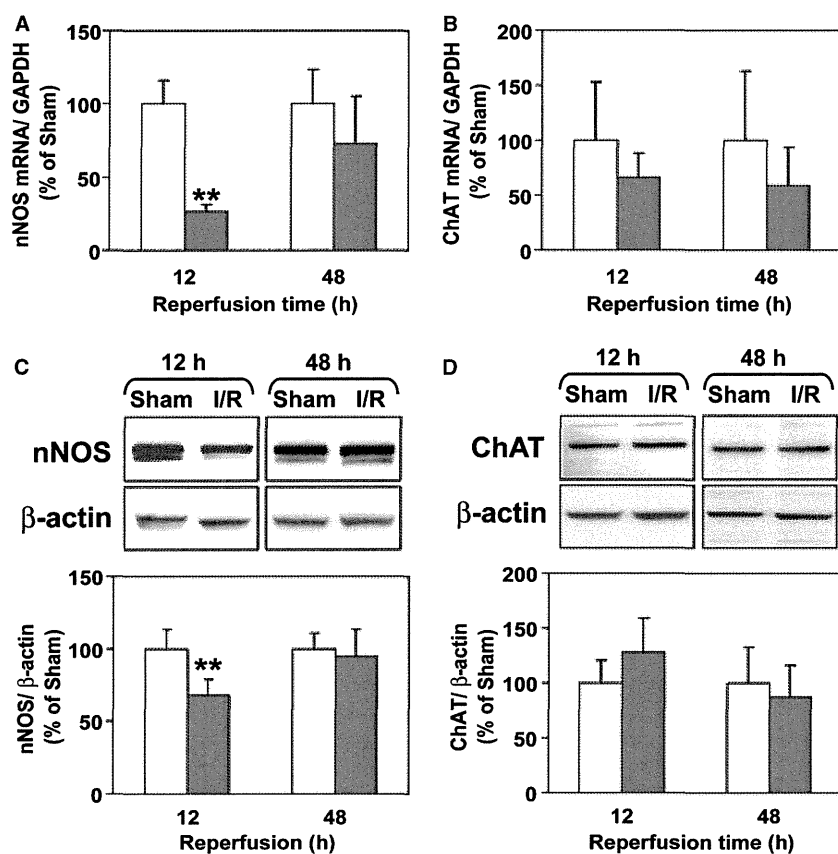


Figure 4 Expression levels of nNOS and ChAT in the stomach of sham-operated rats (open bar) and I/R rats (filled bar) at 12 h (Sham; $n = 6$, I/R; $n = 7$) and 48 h (Sham; $n = 6$, I/R; $n = 7$) after I/R. (A,B) Expression of mRNA as assessed by quantitative RT-PCR. (C,D) Western blot analysis. Data are means \pm SD. ** $P < 0.01$ as compared with sham-operated rats.

Electron microscopy at 12 h after I/R

In the sham-operated rats, cells possessing the typical ultrastructural features of ICC were found in the myenteric plexus region (Fig. 6A) and within the muscle layer. These cells were characterized by an electron-dense cytoplasm, numerous mitochondria and conspicuous caveolae along the cell membrane. They extended long processes containing many mitochondria, rough and smooth endoplasmic reticulum and rich intermediate filaments. The ICC formed gap junctions with each other (Fig. 6B and inset). They were distinguished from fibroblasts by the less electron-dense cytoplasm and well-developed rough endoplasmic reticulum in the latter. In the I/R rats, a decrease in the number of cells that possessed the ultrastructural features of ICC was observed by electron microscopy (Fig. 6C). In such areas, only fibroblasts were observed in the same locations normally occupied by ICC-MY in the regions of the myenteric plexus. Also, no evidence of cell death was observed in these areas. The remaining ICC showed the same ultrastructural features as those in the sham-operated rat, and shared gap junctions with adjacent ICC-IM (Fig. 6D).

DISCUSSION

Thermal injury²⁵ and aspirin ingestion²⁶ have been reported to induce delayed gastric emptying. However, in *Helicobacter pylori* infection, gastric emptying is reportedly accelerated²⁷ or remains unchanged.²⁸ Although these events are reported to be induced by gastric I/R, their influences on the gastric emptying rates varied. Thus, whether acceleration/delay of gastric emptying can be induced by gastric I/R alone remained unclear. The present study is the first report documenting delayed gastric emptying and disruption of neuromuscular components after gastric I/R. In one previous report on the effect of gastric I/R on the gastric motility, increase in the force of contractions after ischaemia was reported, but only for the initial 10 min of reperfusion.²⁹ This was only a short-term evaluation, whereas we performed a longer-term evaluation to investigate the different phases of the motility profile after I/R.

Although dysmotility after intestinal I/R as well as the loss of the ICC network have been reported previously,⁸ no data have been reported on the effect of the gastric I/R on the ICC network in the stomach. This is the first report of disruption of the ICC network

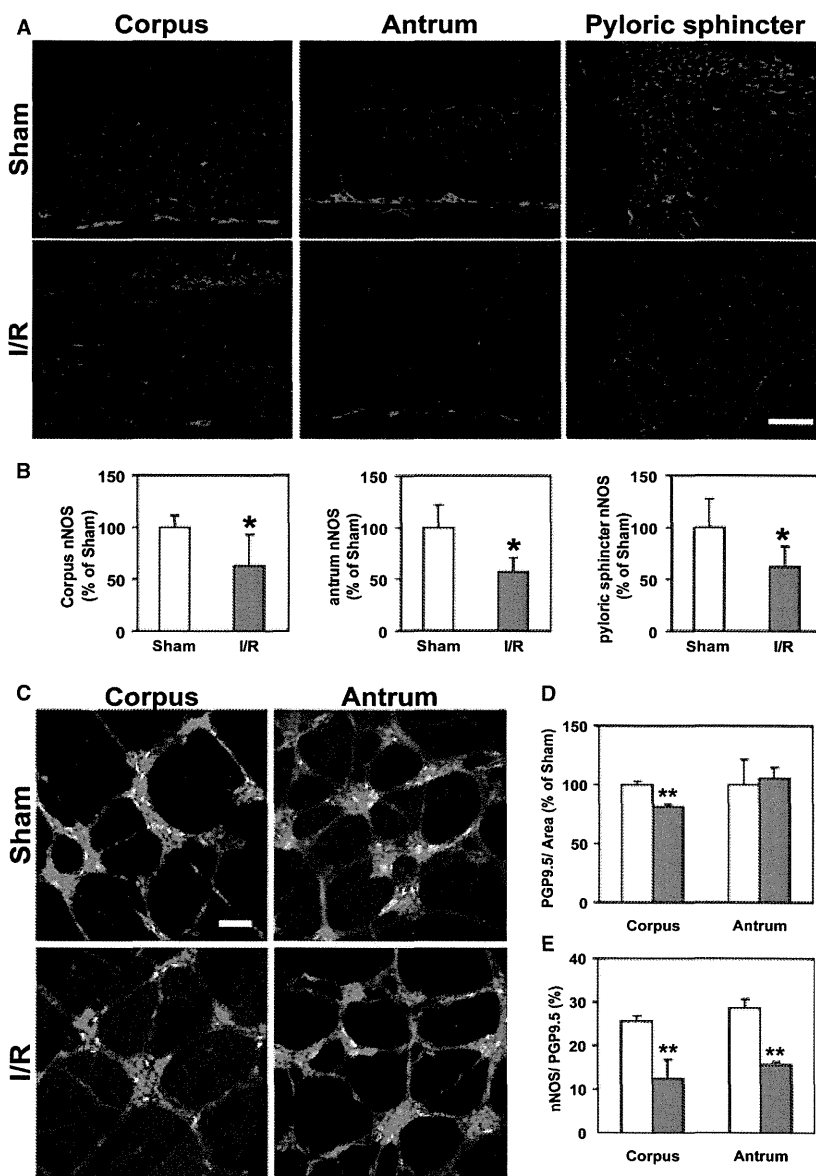


Figure 5 (A) Representative immunofluorescent staining of nNOS in the corpus, antrum and pyloric sphincter of a sham-operated rat and an I/R rat at 12 h. Bar, 100 μ m. (B) Areas of nNOS were quantified using the image analysis software and are shown below the fluorescent images (Sham (open bar); $n = 6$, I/R (filled bar); $n = 7$). Data are means \pm SD. * $P < 0.05$ as compared with sham-operated rats. (C) Representative images of whole-mount immunofluorescent staining for nNOS (red, all of the positive cells are colocalized with PGP9.5 and coloured yellow) and PGP9.5 (green) in the corpus and antrum in a sham-operated rat and an I/R rat at 12 h after I/R. Bar, 100 μ m. (D) Numbers of PGP9.5-immunoreactive cells in each myenteric ganglion normalized by the area of the ganglion. (E) The population of nNOS-positive neurons normalized by the population of PGP9.5-immunoreactive cells. A total of 10 myenteric ganglia were analysed in each preparation [Sham (open bar); $n = 3$, I/R (filled bar); $n = 3$]. Data are means \pm SD. ** $P < 0.01$ as compared with the sham-operated rats.

occurring after gastric I/R in the stomach. Decrease of both ICC-IM and ICC-MY were observed in the corpus, whereas only decrease of the ICC-IM was observed in the antrum at 12 h after I/R (Fig. 3). In patients with type 2 diabetes mellitus and streptozotocin-induced diabetic rats, exclusive decrease of only the ICC-IM was observed in the antrum as compared with that in the controls.^{19,20} Thus, the regulation of ICC-IM may differ from that of ICC-MY. In the present study, loss of ICC (especially ICC-IM together with the decrease in the antral nNOS) might have been involved in the delay of the gastric emptying observed at 12 h after I/R, since these cells mediate nitrergic neuromuscular neurotransmission in the distal stomach. However,

although the gastric emptying was normalized, the loss of ICC in the antrum persisted even at 48 h after I/R (Fig. 3). Changes in gastric emptying associated with I/R could not be explained solely by the observed changes in ICC.

It has been reported that intestinal I/R injury has no effect on the enteric neurons.⁸ However, as concomitant loss of ICC and nNOS are often reported, we examined the effect of gastric I/R on the expression of nNOS and ChAT in this study. Our results indicate a close correlation of the expression of nNOS with the rate of gastric emptying after gastric I/R. The decrease of nNOS expression in the gastric corpus and antrum might have impaired the accommodation reflex and

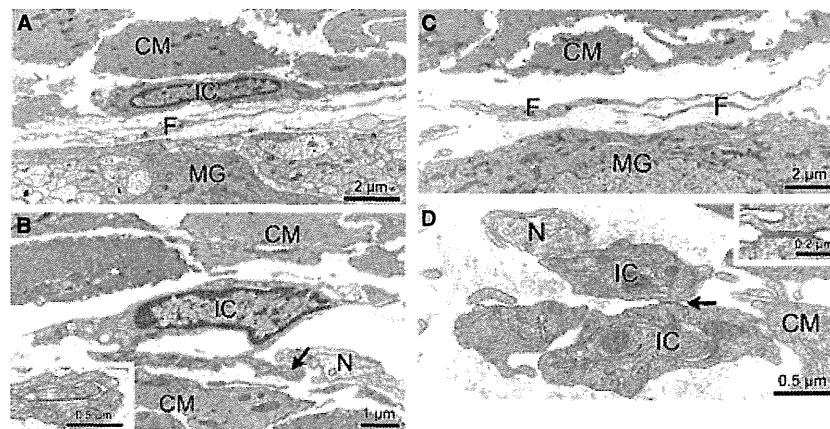


Figure 6 (A–B) Morphology of the tunica muscularis from the corpus of a sham-operated rat. (A) Electron micrographs of the myenteric plexus region. Typical ICC-MY (IC) were observed near the myenteric ganglion (MG), significantly different in appearance from fibroblasts (F). (B) ICC-IM (IC) are closely associated with nerve fibers (N) and shared gap junctions (arrow) with adjacent ICC-IM. Inset: Higher magnification of a gap junction is indicated by the arrow. (C–D) Morphology of the tunica muscularis from the corpus of an I/R rat. (C) Electron micrographs of the myenteric plexus region. Only fibroblasts were observed as the interstitial cells around the myenteric ganglion, and no ICC were observed. (D) The remaining ICC-IM showed the same ultrastructure as that in the sham-operated rats and shared gap junctions (arrow) with adjacent ICC-IM. Inset: Higher magnification of a gap junction indicated by the arrow.

accelerated gastric emptying. However, decreased expression of nNOS in the pyloric sphincter might more potently contribute to the delayed gastric emptying through blockage of the passage of liquid through the pyloric ring (Fig. 5), and a combination of these events might have resulted in a moderate delay of gastric emptying observed after gastric I/R. Transient focal cerebral ischaemia in rats can cause severe damage to nNOS-positive neurons and their eventual death.³⁰ In the present study, a minor, albeit significant decrease in PGP9.5-positive neurons was observed in the corpus after I/R, suggesting possible damage to enteric neurons. However, we did not detect any cell death by the terminal deoxynucleotidyl transferase-mediated dUTP nick end labelling (TUNEL) method (data not shown), and the reduced expression of nNOS was shown to be restored by 48 h after I/R, suggesting differential effects of I/R on nNOS-positive neurons in the stomach and cerebrum. Proteins, including PGP9.5, in the nNOS-positive neurons might have been transiently downregulated after I/R in the corpus. As hypoxia has been reported to rather increase nNOS expression,³¹ the reduction of nNOS expression after I/R observed in the present study might have occurred in the reperfusion stage. I/R-induced production and release of proinflammatory interferon- γ ³² and platelet-activating factor³³ might contribute to the reduced expression of nNOS.^{34,35}

In the present study, concomitant decrease in the number of nNOS and ICC was observed in the corpus at 12 h, and then restored at 48 h after I/R (Figs 3 and 4). According to the report by Choi *et al.*,³⁶ significant

reduction of the c-Kit immunoreactive networks of ICC from nNOS-deficient mice was observed as compared with that in the control mice and the number of ICC in organotypic cultures increased by an NO donor and decreased by an NOS inhibitor, suggesting that nNOS-derived NO is important for the presence of ICC in the gastrointestinal tract. In contrast, the distribution of NOS-containing nerves were unaffected by the absence of ICC in *W/W^v* animals.³⁷ Thus, reduction in the number of nNOS-positive neurons might be involved in the loss of ICC in the corpus after I/R. However, as the lack of temporal correlation between the reduced nNOS and c-Kit expression has been reported in non-obese diabetic (NOD) mice,³⁸ a common factor might have induced the simultaneous loss of both the ICC and nNOS-positive neurons. Oxidative stress produced by the xanthine–xanthine oxidase system after I/R may have played a major role in the disruption of the ICC network in this model, as oxidative stress associated with diabetes has been reported to induce a reduction of c-Kit expression and ICC damage.³⁸ Disruption of the ICC in the antrum persisted until 48 h after I/R, at which point the nNOS expression was restored. It appears that the recovery of the ICC network in the antrum might take longer as compared with that in the corpus. The decrease in the expression of membrane-bound SCF at 12 and 48 h after I/R in the present study (Fig. 2) might have also contributed to the delayed recovery of the ICC in the antrum, as reported for studies of diabetic *db/db* mice and NOD mice,^{39,40} although the contribution might have been small in this acute model of gastric I/R. The

differential effect of I/R on the ICC in the corpus and antrum still remains to be elucidated.

The ultrastructural analysis revealed a marked decrease in the number of cells with typical ICC morphology at 12 h after I/R (Fig. 6). These results indicate that the reduction in c-Kit protein observed after I/R probably reflected true loss of ICC. Apoptosis of ICC has been reported to be detected after intestinal ischaemia for 60 min and reperfusion for 12 h by TUNEL method.⁴¹ However, we did not detect apoptosis by the same method after gastric ischaemia for 80 min and reperfusion for 12 h and no characteristic findings of cell death were detected by electron microscopy. There is a possibility that the apoptotic ICC were already phagocytosed by 12 h after I/R in the stomach. However, since the ICC in the corpus were restored by 48 h after I/R, it is unlikely that the gastric ICC undergo apoptosis after gastric I/R. According to a previous report, under the condition of blockade of the

c-Kit pathway, the ICC phenotype changes toward a more smooth muscle-like phenotype.⁴² In the present study, we did not detect any intermediate phenotype by electron microscopy at 12 h after I/R. Although the ICC might have undergone complete transition to smooth muscle cells, further investigation is awaited to clarify the exact fate of the ICC after I/R.

In conclusion, delayed gastric emptying was observed after gastric I/R, with a significant decrease in the number of ICC and nNOS-positive neurons. These results suggest that the rat model of gastric ischaemia and reperfusion is a convenient model of acute gastroparesis that shows a similar pathology to diabetic gastroparesis.

CONFLICT OF INTEREST

No conflicts of interest exist.

REFERENCES

- Kitajima M, Otsuka S, Shimizu A *et al.* Impairment of gastric microcirculation in stress. *J Clin Gastroenterol* 1988; **10**(Suppl. 1): S120–8.
- Zinner MJ, Turtinen L, Gurl NJ. The role of acid and ischemia in production of stress ulcers during canine hemorrhagic shock. *Surgery* 1975; **77**: 807–16.
- Takeuchi K, Ueshima K, Hironaka Y, Fujioka Y, Matsumoto J, Okabe S. Oxygen free radicals and lipid peroxidation in the pathogenesis of gastric mucosal lesions induced by indomethacin in rats. Relation to gastric hypermotility. *Digestion* 1991; **49**: 175–84.
- Suzuki H, Hibi T, Marshall BJ. *Helicobacter pylori*: present status and future prospects in Japan. *J Gastroenterol* 2007; **42**: 1–15.
- Suzuki H, Suzuki M, Imaeda H, Hibi T. *Helicobacter pylori* and microcirculation. *Microcirculation* 2009; **16**: 547–58.
- Udassin R, Eimerl D, Schiffman J, Haskel Y. Postischemic intestinal motility in rat is inversely correlated to length of ischemia. An *in vivo* animal model. *Dig Dis Sci* 1995; **40**: 1035–8.
- Takahashi A, Tomomasa T, Kaneko H *et al.* Intestinal motility in an *in vivo* rat model of intestinal ischemia-reperfusion with special reference to the effects of nitric oxide on the motility changes. *J Pediatr Gastroenterol Nutr* 2001; **33**: 283–8.
- Shimajima N, Nakaki T, Morikawa Y *et al.* Interstitial cells of Cajal in dysmotility in intestinal ischemia and reperfusion injury in rats. *J Surg Res* 2006; **135**: 255–61.
- Huizinga JD, Thuneberg L, Kluppel M, Malysz J, Mikkelsen HB, Bernstein A. W/kit gene required for interstitial cells of Cajal and for intestinal pacemaker activity. *Nature* 1995; **373**: 347–9.
- Ward SM, Burns AJ, Torihashi S, Sanders KM. Mutation of the proto-oncogene c-kit blocks development of interstitial cells and electrical rhythmicity in murine intestine. *J Physiol* 1994; **480** (Pt 1): 91–7.
- Torihashi S, Ward SM, Sanders KM. Development of c-Kit-positive cells and the onset of electrical rhythmicity in murine small intestine. *Gastroenterology* 1997; **112**: 144–55.
- Ward SM, Harney SC, Bayguinov JR, McLaren GJ, Sanders KM. Development of electrical rhythmicity in the murine gastrointestinal tract is specifically encoded in the tunica muscularis. *J Physiol* 1997; **505**(Pt 1): 241–58.
- Sanders KM. A case for interstitial cells of Cajal as pacemakers and mediators of neurotransmission in the gastrointestinal tract. *Gastroenterology* 1996; **111**: 492–515.
- Burns AJ, Lomax AE, Torihashi S, Sanders KM, Ward SM. Interstitial cells of Cajal mediate inhibitory neurotransmission in the stomach. *Proc Natl Acad Sci USA* 1996; **93**: 12008–13.
- Ward SM, Beckett EA, Wang X, Baker F, Khoyi M, Sanders KM. Interstitial cells of Cajal mediate cholinergic neurotransmission from enteric motor neurons. *J Neurosci* 2000; **20**: 1393–403.
- He CL, Soffer EE, Ferris CD, Walsh RM, Szurszewski JH, Farrugia G. Loss of interstitial cells of Cajal and inhibitory innervation in insulin-dependent diabetes. *Gastroenterology* 2001; **121**: 427–34.
- Watkins CC, Sawa A, Jaffrey S *et al.* Insulin restores neuronal nitric oxide synthase expression and function that is lost in diabetic gastropathy. *J Clin Invest* 2000; **106**: 373–84.
- Ordog T, Takayama I, Cheung WK, Ward SM, Sanders KM. Remodeling of networks of interstitial cells of Cajal in a murine model of diabetic gastroparesis. *Diabetes* 2000; **49**: 1731–9.
- Iwasaki H, Kajimura M, Osawa S *et al.* A deficiency of gastric interstitial cells of Cajal accompanied by decreased expression of neuronal nitric oxide synthase and substance P in patients with type 2 diabetes mellitus. *J Gastroenterol* 2006; **41**: 1076–87.

- 20 Wang XY, Huizinga JD, Diamond J, Liu LW. Loss of intramuscular and submuscular interstitial cells of Cajal and associated enteric nerves is related to decreased gastric emptying in streptozotocin-induced diabetes. *Neurogastroenterol Motil* 2009; **21**: 1095–e92.
- 21 Takahashi T. Pathophysiological significance of neuronal nitric oxide synthase in the gastrointestinal tract. *J Gastroenterol* 2003; **38**: 421–30.
- 22 Babbedge RC, Bland-Ward PA, Hart SL, Moore PK. Inhibition of rat cerebellar nitric oxide synthase by 7-nitroindazole and related substituted indazoles. *Br J Pharmacol* 1993; **110**: 225–8.
- 23 Mashimo H, Kjellin A, Goyal RK. Gastric stasis in neuronal nitric oxide synthase-deficient knockout mice. *Gastroenterology* 2000; **119**: 766–73.
- 24 Kido T, Nakai Y, Kase Y *et al.* Effects of rikkunshi-to, a traditional Japanese medicine, on the delay of gastric emptying induced by N(G)-nitro-L-arginine. *J Pharmacol Sci* 2005; **98**: 161–7.
- 25 Iseri SO, Gedik IE, Erzik C *et al.* Oxytocin ameliorates skin damage and oxidant gastric injury in rats with thermal trauma. *Burns* 2008; **34**: 361–9.
- 26 Shea-Donohue T, Steel L, Montcalm-Mazzilli E, Dubois A. Aspirin-induced changes in gastric function: role of endogenous prostaglandins and mucosal damage. *Gastroenterology* 1990; **98**: 284–92.
- 27 Sykora J, Malan A, Zahlava J *et al.* Gastric emptying of solids in children with *H. pylori*-positive and *H. pylori*-negative non-ulcer dyspepsia. *J Pediatr Gastroenterol Nutr* 2004; **39**: 246–52.
- 28 Chiloiro M, Russo F, Riezzo G *et al.* Effect of *Helicobacter pylori* infection on gastric emptying and gastrointestinal hormones in dyspeptic and healthy subjects. *Dig Dis Sci* 2001; **46**: 46–53.
- 29 Wood JG, Yan ZY, Zhang Q, Cheung LY. Ischemia-reperfusion increases gastric motility and endothelin-1-induced vasoconstriction. *Am J Physiol* 1995; **269**: G524–31.
- 30 Sakuma M, Hyakawa N, Kato H, Araki T. Time dependent changes of striatal interneurons after focal cerebral ischemia in rats. *J Neural Transm* 2008; **115**: 413–22.
- 31 Ward ME, Toporsian M, Scott JA *et al.* Hypoxia induces a functionally significant and translationally efficient neuronal NO synthase mRNA variant. *J Clin Invest* 2005; **115**: 3128–39.
- 32 Osman M, Russell J, Granger DN. Lymphocyte-derived interferon-gamma mediates ischemia-reperfusion-induced leukocyte and platelet adhesion in intestinal microcirculation. *Am J Physiol Gastrointest Liver Physiol* 2009; **296**: G659–63.
- 33 Yoshikawa T, Takahashi S, Naito Y *et al.* Effects of a platelet-activating factor antagonist, CV-6209, on gastric mucosal lesions induced by ischemia-reperfusion. *Lipids* 1992; **27**: 1058–60.
- 34 Bandyopadhyay A, Chakder S, Rattan S. Regulation of inducible and neuronal nitric oxide synthase gene expression by interferon-gamma and VIP. *Am J Physiol* 1997; **272**: C1790–7.
- 35 Qu XW, Wang H, Rozenfeld RA, Huang W, Hsueh W. Type I nitric oxide synthase (NOS) is the predominant NOS in rat small intestine. Regulation by platelet-activating factor. *Biochim Biophys Acta* 1999; **1451**: 211–7.
- 36 Choi KM, Gibbons SJ, Roeder JL *et al.* Regulation of interstitial cells of Cajal in the mouse gastric body by neuronal nitric oxide. *Neurogastroenterol Motil* 2007; **19**: 585–95.
- 37 Ward SM, Morris G, Reese L, Wang XY, Sanders KM. Interstitial cells of Cajal mediate enteric inhibitory neurotransmission in the lower esophageal and pyloric sphincters. *Gastroenterology* 1998; **115**: 314–29.
- 38 Choi KM, Gibbons SJ, Nguyen TV *et al.* Heme oxygenase-1 protects interstitial cells of Cajal from oxidative stress and reverses diabetic gastroparesis. *Gastroenterology* 2008; **135**: 2055–64, 2064 e2051–2052.
- 39 Yamamoto T, Watabe K, Nakahara M *et al.* Disturbed gastrointestinal motility and decreased interstitial cells of Cajal in diabetic db/db mice. *J Gastroenterol Hepatol* 2008; **23**: 660–7.
- 40 Horvath VJ, Vittal H, Lorincz A *et al.* Reduced stem cell factor links smooth myopathy and loss of interstitial cells of cajal in murine diabetic gastroparesis. *Gastroenterology* 2006; **130**: 759–70.
- 41 Mei F, Guo S, He YT *et al.* Apoptosis of interstitial cells of Cajal, smooth muscle cells, and enteric neurons induced by intestinal ischemia and reperfusion injury in adult guinea pigs. *Virchows Arch* 2009; **454**: 401–9.
- 42 Torihashi S, Nishi K, Tokutomi Y, Nishi T, Ward S, Sanders KM. Blockade of kit signaling induces transdifferentiation of interstitial cells of cajal to a smooth muscle phenotype. *Gastroenterology* 1999; **117**: 140–8.

Post-infectious Functional Dyspepsia - A Novel Disease Entity among Functional Gastrointestinal Disorders - Relation to *Helicobacter pylori* Infection?

(Neurogastroenterol Motil 2009;21:832-e56)

Hidekazu Suzuki, M.D., Ph.D.

Division of Gastroenterology and Hepatology, Department of Internal Medicine, Keio University School of Medicine, Tokyo, Japan

Summary

Kindt et al.¹ published a report entitled "Intestinal immune activation in presumed post-infectious functional dyspepsia" in the August issue of Neurogastroenterology and Motility in 2009. By comparing the signs of inflammation and the degree of hyperplasia of the enterochromaffin cells (EC) in duodenal biopsies obtained from patients with presumed post-infectious functional dyspepsia (PI-FD) and unspecified-onset functional dyspepsia (U-FD), they showed that PI-FD is associated with persistence of focal T-cell aggregates, decrease in CD4⁺ cells and increased macrophage counts surrounding the crypts, without any significant differences in the numbers of EC or chromogranin A (CA)-positive cells (mast cells). This finding may indicate impaired ability of the immune system in these cases to terminate the inflammatory response after an acute insult.

Comment

In irritable bowel syndrome (IBS), a post-infectious disease entity was reported in 1962 by Chaudhary and Truelove, who showed that 23% of IBS patients gave a history of an episode of bacillary or amoebic dysentery.² Ever since, an increasing number of studies have reported on the development of post-infectious IBS.

In relation to PI-FD, Mearin et al.³ reported a significantly increased prevalence of FD up to 1 year after an outbreak of Salmonella gastroenteritis. In PI-FD patients, early satiety, weight loss, nausea, and vomiting are more frequently reported, while gastric sensorimotor function testing revealed a particularly high prevalence of impaired gastric accommodation.⁴ In the study by Kindt et al.,¹ the focal aggregates of CD8⁺ T cells, decrease in CD4⁺ T cells and increased macrophage counts surrounding the duodenal crypts persisted for several months after the acute infectious episodes, suggesting delay or impairment of termination of the inflammatory response even after adequate re-

Received: November 17th, 2009 Accepted: November 24th, 2009

© This is an Open Access article distributed under the terms of the Creative Commons Attribution Non-Commercial License (<http://creativecommons.org/licenses/by-nc/3.0>) which permits unrestricted non-commercial use, distribution, and reproduction in any medium, provided the original work is properly cited.

*Correspondence: Hidekazu Suzuki, M.D., Ph.D.

Department of Internal Medicine, Keio University School of Medicine, 35 Shinanomachi, Shinjuku-ku, Tokyo 160-8582, Japan
Tel: +81-3-5363-3914, Fax: +81-3-5363-3967, E-mail: hsuzuki@sc.itc.keio.ac.jp

Financial support: This study was supported by the Keio Gijuku Academic Development Funds (to H.S.).

Conflicts of interest: None.